Single-cell DNA sequencing has revealed the evolution of resistant clones to Third-generation EGFR-TKIs in non-small cell lung cancer

Mina Han

The Graduate School
Yonsei University
Department of Medicine

Single-cell DNA sequencing has revealed the evolution of resistant clones to Third-generation EGFR-TKIs in non-small cell lung cancer

A Master's Thesis Submitted
to the Department of Medicine
and the Graduate School of Yonsei University
in partial fulfillment of the
requirements for the degree of
Master of Medical Science

Mina Han

December 2024

This certifies that the Master's Thesis of Mina Han is approved

Thesis Supervisor Hye Ryun Kim

Thesis Committee Member Sangwoo Kim

Thesis Committee Member Hyo Sup Shim

The Graduate School
Yonsei University
December 2024

TABLE OF CONTENTS

LIST OF FIGURES

LIST OF TABLES

ABSTRACT

Single-cell DNA sequencing has revealed the evolution of resistant clones to Third-generation EGFR-TKIs in non-small cell lung cancer

Third-generation EGFR-TKIs, such as targeted agents, have significantly improved patient outcomes, but drug resistance inevitably develops. In non-small cell lung cancer (NSCLC) resistant to third-generation EGFR-TKIs, genetic alterations, including *MET*, *ERBB2*, and *EGFR* C797S, have been reported, and there is ongoing debate regarding whether resistance mechanisms occur mutually exclusively or if oncogenic *EGFR* mutations are acquired. We investigated genetic heterogeneity in 49 patients with advanced *EGFR*-mutant NSCLC at baseline and after developing resistance using next-generation sequencing (NGS). To determine whether resistance-associated mutations and activating *EGFR* mutations coexist within a single cancer cell or arise in distinct cell populations, we performed single-cell DNA sequencing (scDNA-seq) on tumor samples from five patients with disease progression on third-generation EGFR-TKIs. Furthermore, osimertinib-resistant cell lines were established, and subjected to scDNA-seq, and the identified mutations were functionally characterized through in vitro experiments. Single-cell analysis revealed that *EGFR*-dependent somatic mutations arise within *EGFR* oncogenic clones, while *EGFR*-independent mutations with low variant allele frequencies occur mutually exclusively. Furthermore, somatic mutations and multiple copy number alterations emerged at distinct spatial and temporal points during treatment with third-generation EGFR-TKIs. This study highlights the genetic heterogeneity, clonal evolution, and spatial distribution patterns of tumor cells associated with resistance to third-generation EGFR-TKIs. These findings provide a rationale for combination therapy intensification in managing *EGFR*-mutant NSCLC patients.

Keywords: NSCLC, EGFR-TKI, Single-cell DNA-seq

I. INTRODUCTION

Lung cancer is the most prevalent cause of cancer-related mortality globally, with non-small cell lung cancer (NSCLC) making up around 85% of reported cases[1]. Activating mutations in the epidermal growth factor receptor (*EGFR*) gene, predominantly exon 19 deletions (E19del) and exon 21 L858R point mutations (L858R), account for approximately 90% of genetic alterations in NSCLC[2, 3]. Third-generation *EGFR* tyrosine kinase inhibitors (TKIs) were initially approved as second-line or later-line treatments for *EGFR*-mutant lung cancer patients with *EGFR* T790M mutations following disease progression on prior EGFR-TKIs. Currently, osimertinib and lazertinib have demonstrated significant improvements in overall survival (OS) and are now established as the standard of care for first-line treatment[4-7]. While third-generation EGFR-TKIs offer substantial survival benefits, the inevitable development of acquired resistance remains a significant challenge, ultimately resulting in disease progression[8].

Resistance development and progression in *EGFR* mutant lung cancer typically follow at least two major pathways: *EGFR*-dependent or bypass signaling mechanisms[9, 10]. *EGFR*-dependent pathways include alterations such as *EGFR* C797S mutation and *EGFR* amplification (amp), while bypass signaling pathways such as *EGFR*-independent pathways involve Mesenchymal-Epithelial Transition (*MET*) amp, *ERBB2* amp, *PIK3CA* mutation, and small cell lung cancer (SCLC) transformation8. As resistance mechanisms have been increasingly elucidated, studies have focused on developing tailored follow-up treatments based on specific biomarkers, highlighting the importance of customized therapy[11]. Studies are evaluating MET-TKIs for *MET* amp following osimertinib and combination therapies, such as erlotinib and osimertinib, for *EGFR* C797S mutations[12-14]. Despite these advancements, unidentified resistance mechanisms remain responsible for 40–65% of cases, necessitating further investigation[9, 15].

Acquired resistance mutations arising during EGFR-TKI therapy have been extensively studied. However, it remains unclear whether these TKI resistance mechanisms occur within the same cell clones harboring *EGFR* activating mutations, representing an accumulation process, or arise in distinct cell populations. Elucidating the distribution patterns of acquired resistance mutations and original *EGFR* activating mutations at the single-cell level is expected to provide valuable insights for developing subsequent therapeutic strategies in patients with *EGFR*-TKI resistance[15, 16].

In this study, we propose utilizing single-cell multi-omics analysis to explore disease progression and gain insights into clonal evolution and the genomic alterations associated with disease progression and therapeutic response. By characterizing genetic changes at the single-cell level, we aim to elucidate the clonal evolution that underlies tumor heterogeneity, ultimately facilitating the development of innovative therapeutic options to address resistance mechanisms.

II. Methods

2.1. Next Generation Sequencing

Genomic DNA and RNA were extracted from formalin-fixed, paraffin-embedded (FFPE) tissue using the AllPrep DNA/RNA FFPE Kit (Qiagen, Hilden, Germany, Cat# 80234), following the manufacturer's instructions. The TruSight Oncology 500 gene panel (Illumina, San Diego, CA, USA) was employed for library preparation and hybrid capture of 523 genes and 55 transcripts from the DNA and RNA samples, respectively. Each sample underwent sequencing with the NextSeq 550Dx System (Illumina), resulting in FASTQ files. Variant calling was conducted using the TruSight Oncology 500 Local App (Illumina, version 1.3), which included pipelines for analyzing the FASTQ files derived from DNA and RNA samples.

2.2. Single-cell DNA-sequencing and Analysis

2.2.1. Sample preparation for Single-cell DNA sequencing

We determined that samples were required to evaluate the resistance mechanisms against third-generation *EGFR-TKIs*. For patients with *EGFR*-mutant NSCLC receiving these medications, tissue samples were collected from those who encountered disease progression. These patients underwent surgical resection at Severance Hospital in Seoul, South Korea, from May 2022 to August 2023. The study received approval from the Institutional Review Board at Severance Hospital, and all patients provided written informed consent to participate.

On the day of surgery, we collected fresh tumors and dissociated tissues using a gentleMACS dissociator (Miltenyi Biotec, Bergisch Gladbach, Germany, Cat# 130-093-235) and the Human Tumor Dissociation Kit (Miltenyi Biotec, Cat# 130-095-929), adhering to the manufacturer's protocol. After incubating for one hour at 37°C, we filtered the resuspended samples through a 70μm MACS SmartStrainer (Miltenyi Biotec, Cat# 130-098-462) into RPMI-1640 medium (Corning, Cat# 10-040-CV) supplemented with 10% fetal bovine serum (FBS, Gibco, Cat# 16000-044) and 1% Penicillin-Streptomycin (Gibco, Cat# 15140122). The filtered samples underwent centrifugation at 1800 rpm for 8 minutes. We then suspended the pellet in ACK lysing buffer (Gibco, Cat# A1049201) for 3 minutes at room temperature. Following lysis, we added RPMI-1640 medium with 10% FBS

and 1% penicillin-streptomycin and centrifuged again at 1800 rpm for 8 minutes.

2.2.2. Single-cell DNA Sequencing

Cell counts and viability were assessed using a Countess Automated Cell Counter (Thermo Fisher Scientific, USA). Following the manufacturer's guidelines, samples were diluted, and about 50,000-76,000 cells/ml were prepared for the Tapestri Instrument (Mission Bio) for processes including encapsulation, lysis, and protein digestion. Single-cell DNA libraries were created using the Mission Bio Tapestri Single-Cell DNA THP Panel (Mission Bio, USA).

2.2.3. Single-Nucleotide Variant Filtering

Mission Bio's Tapestri Pipeline processed the sequencing data. Subsequently, the data were analyzed with Mission Bio's Tapestri Insights software package (Version 2.2) and visualized using R software (Version 4.1). The proprietary Tapestri analysis pipeline integrated data pre-processing for variant discovery. Six filter parameters were used to exclude low-quality cells and variants: (1) removal of genotypes from cells with quality scores < 30; (2) removal of genotypes from cells with read depths < 10; (3) removal of genotypes from cells with alternate allele frequencies < 20; (4) removal of variants genotyped in < 50% of cells; (5) removal of cells with < 50% of genotypes present; and (6) removal of variants mutated in < 0.3% of cases cells.

2.2.4. Single-Nucleotide Variant Calling

Initially, we eliminated polymorphic variants identified in all samples to pinpoint the final pathogenic somatic variants. Next, we chose variants based on specific criteria: (1) the variant allele frequency (VAF) must exceed 0.01 in over 1% of cells, (2) the minimum VAF by cell count among mutated cells should be at least 0.3, and (3) the VAF by Cell Count must be greater than the VAF by Read Count by more than 1.5-fold. We manually reviewed these selected variants, retaining only exon variants. From this high-quality set, we picked non-intronic somatic variants for further analysis. The *DANN* scoring system was utilized as the first filtering step to evaluate the pathogenicity of each variant, applying a cutoff *DANN* score of ≤0.95 to exclude non-pathogenic variants[17]. Pathogenic variants are classified based on two criteria: they either lead to a biological loss of function (such as missense, nonsense, or they are documented as pathogenic in clinical

databases like CLINVAR and COSMIC and Varsome[18]) and have strong evidence of pathogenicity from in silico prediction tools. Upon filtering, we concentrated solely on the identified pathogenic variants by removing common variants in the human population (frequency > 1%) and keeping only those variants with verified evidence of pathogenicity in extensive clinical assessment databases.

2.2.5. Copy Number Variants Analysis

The copy number analysis primarily used Mission Bio's Mosaic package, version 3.4. Read counts for each amplicon were normalized to correct for systematic artifacts. This normalization occurred within the same cell across different amplicons by calculating the mean read depth and then within the same amplicon across various cells by determining the median read depth. It's essential to note that the median read depth is deemed high-quality only in cells with at least one-tenth the number of reads compared to the cell ranked 10th in read count. This normalization step was executed using the "normalize_reads" method from the Mosaic package.

The per-amplicon ploidy was determined by setting a diploid baseline using a group of cells, guided by existing knowledge, such as the *EGFR* mutational status. Subsequently, the read counts per amplicon for each cell were compared against the median read count of this baseline group count.

We categorized the scDNA-seq library into *EGFR*-mutated and *EGFR*-wild type (WT) clones, mainly representing normal cells. We removed cells from the *EGFR* WT clones containing the pathogenic somatic mutation identified. We converted the normalized reads into copy number estimates by assuming the WT clone identified through mutation analysis is diploid. The counts of all other cells were scaled to match this WT clone's counts, which were normalized to read count to calculate the copy number estimates.

Cells were grouped according to the variant classifications, with per-gene copy number alterations (CNAs) identified for each clone only when more than two amplicons of a specific gene showed an amplified (CN > 2.2) or deleted (CN < 1.0) copy number signal[19, 20].

2.3. Cell Line Experiments

2.3.1. Cell Cultures

All NSCLC cell lines were cultured in RPMI-1640 medium supplemented with 10% FBS and 1% penicillin-Streptomycin at 37℃ and 5% CO2 in a humidified incubator. The cells were sub-cultured

every 2-3 days after reaching 80% confluency. All reference compounds were obtained from Selleckchem.

2.3.2. Establish Osimertinib Resistance Cell Line

Cell lines were initiated with 10 nM osimertinib in RPMI 1640 medium enriched with 10% FBS and 1% penicillin-Streptomycin. We established human *EGFR*-mutant NSCLC cell lines (NCI-H1975, HCC827) with acquired resistance by gradually increasing the osimertinib dosage to 1 μM over five months. After treatment, the osimertinib-exposed cell lines were kept for an additional month, during which they maintained comparable growth rates to the parent cell lines, proliferating without significant cell death. The resulting resistant cell lines, H1975OR and HCC827OR, demonstrate resistance to osimertinib.

2.3.3. Cell Viability Assay and Crystal Violet Staining

Cells were inoculated into flat-bottom 96-well plates (Corning, Cat# 3595) at a density of $5x10^3$ cells per well, in either triplicate or quadruplicate. Following overnight incubation, the cells were cultured with or without osimertinib, erdafitinib, and ruxolitinib at various concentrations for 72 hours in RPMI 1640 medium supplemented with 2% FBS and 1% penicillin-Streptomycin. The drugs were diluted serially. In control wells, dimethyl sulfoxide (Sigma, Cat# D2650) was incorporated at the highest dilution from the assay. Cell viability was measured using an ez-cytox assay (DogenBio, Cat# ez-3000). For each well, a volume of ez-cytox reagent equal to 1/10 of the cell culture medium was added, and the plate was incubated for at least 2H 30 minutes before measuring the absorbance.

Next, the solution was aspirated, and the cells were rinsed with Dulbecco's Phosphate -Buffered Salines (D-PBS, Welgene, Cat# LB001-02). The cells were fixed in cold methanol for 10 minutes. After fixation, they were stained with 0.1% crystal violet for 10 minutes at room temperature. The dye was then rinsed off using PBS, and the areas were scanned after drying. Data were analyzed and plotted with PRISM 8.0.

2.4. Statistical analysis

Clonal prevalence and Phylogenetic trees were created utilizing the "timescape" package with R

version 4.3.1.

III. Results

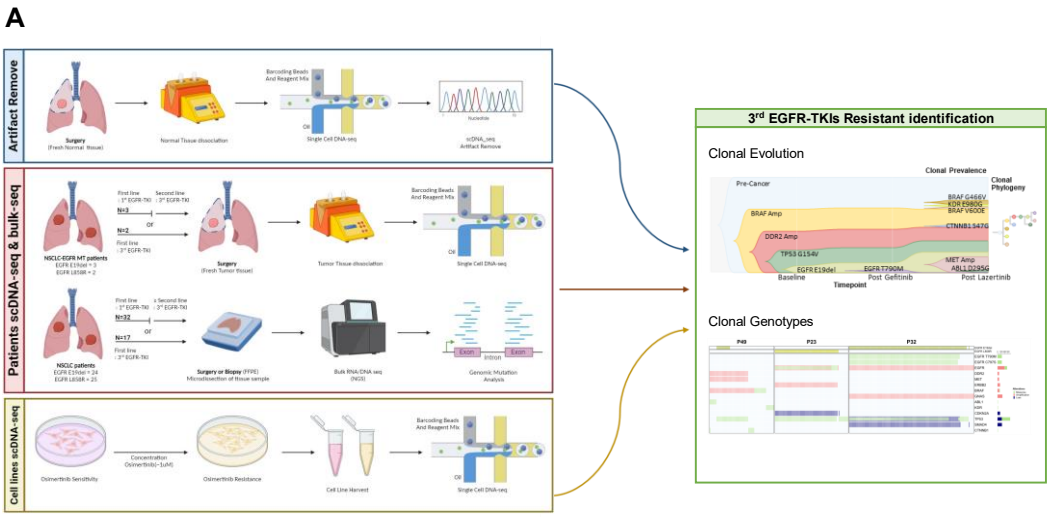

Figure 1. Study design of patients with third-generation EGFR-TKIs resistance.

A. Summary of the procedure used in this study.

3.1. Workflow to Analyze Resistance to Third-generation EGFR-TKIs in Patients' Tumor Tissue and In vitro.

To identify genetic resistance mechanisms in patients, we conducted bulk-sequencing (seq) using formalin-fixed, paraffin-embedded (FFPE) samples from 49 patients treated with third-generation EGFR-TKIs, analyzing each genomic alteration. Sequencing results revealed different resistance mechanisms across patients. After identifying that the mutation frequencies varied among individual patients, we conducted single-cell DNA sequencing (scDNA-seq) on fresh surgical tumor tissue from five patients treated with third-generation EGFR-TKIs to elucidate how intra-tumoral heterogeneity arises at the single-cell level. Additionally, scDNA-seq was executed on the same panel after establishing osimertinib-resistant cell lines. In vitro experiments were then performed to study functionally identified acquired mutations (Figure 1A, Supplementary Figure 1A).

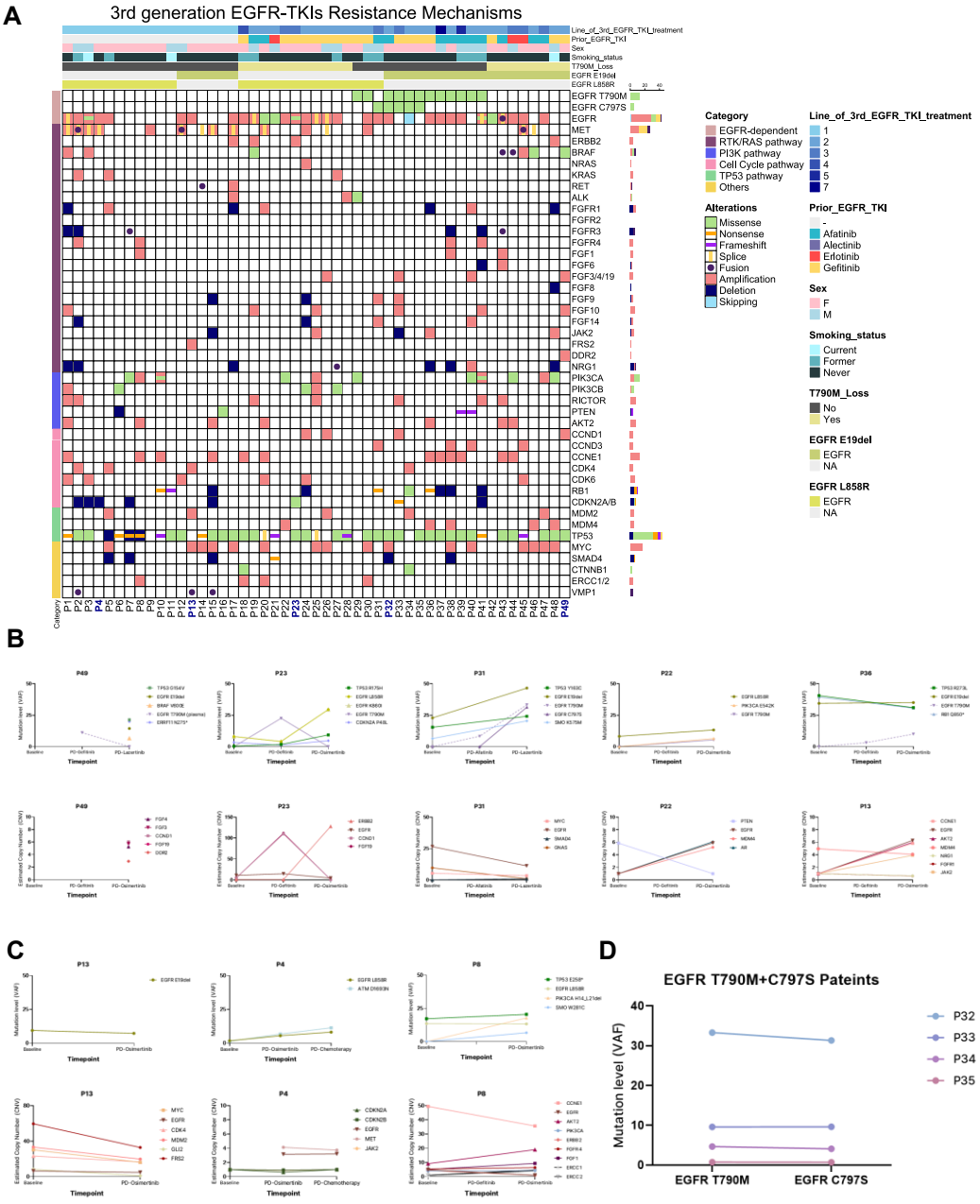

Figure 2. Genetic landscape of third-generation EGFR-TKIs progression status from EGFR mutant NSCLC patients.

A. Oncoplot of SNVs and CNVs in third-generation EGFR-TKIs progression in 49 patient samples. B-C. Change VAFs in SNVs and CNVs during third-generation EGFR-TKIs treatment in (B) ≥ second-line patients and (C) first-line patients The Y-axis indicates VAFs or CNVs for mutations or genes, and the X-axis indicates the clinical timepoints. *EGFR* T790M, expressed in dotted lines, is the result obtained from Liquid biopsy. D. Changes in *EGFR*-dependent mutations VAF during EGFR-TKIs treatment. The Y-axis indicates VAF for mutations, and the X-axis indicates *EGFR* T790M and C797S mutations.

CNV, copy number variant; EGFR, epidermal growth factor receptor; SNV, single nucleotide variant; TKI, tyrosine kinase inhibitor; VAF, variant allele frequency.

3.2. The Genetic Landscape of Third-generation EGFR-TKIs

To characterize the resistance mechanisms associated with third-generation EGFR-TKI therapy, we conducted bulk-seq of 523 genes using FFPE tissue samples from 49 patients who experienced disease progression. An overview of patient characteristics are summarized in Table 1. Patients ' median age at diagnosis was 61 years (range: 33–81), with 67% of the patients being female and 74% having no smoking history. All patients were diagnosed with adenocarcinoma, and at the initiation of third-generation EGFR-TKI treatment, 59% had brain metastases. Thirty-five percent of the patients received first-line treatment with third-generation EGFR-TKIs, whereas 65% had already experienced between one and six lines of prior treatment. Of these earlier therapies, 38% of patients received afatinib, 9% erlotinib, and 53% gefitinib. The predominant *EGFR* mutations were E19dels (49%) and the L858R point mutation (51%). Among those receiving treatment beyond the second line, 31 (97%) presented with the T790M mutation before starting third-generation EGFR-TKI treatment.

The landscape of genomic alterations identified in samples obtained after third-generation EGFR-TKI treatment is shown in Figure 2A. The most prevalent acquired resistance mechanism was the loss of the *EGFR* T790M mutation, which occurred in 60% of patients, excluding those with *EGFR* oncogenic and *TP53* mutations. This was followed by *PIK3CA* mutations (16%), *PIK3CB* mutations (6%), and *BRAF* mutations (6%). Excluding *EGFR* amp, the identified changes in copy number alterations (CNAs) were associated with the receptor tyrosine kinase (RTK)-RAS pathway (63%), the Phosphatidylinositol-3-kinase (PI3K) pathway (24%), the cell cycle pathway (51%), the *TP53* pathway (24%), and other pathways (40%).

As previously reported[8, 21], our data has also observed copy number variations (CNVs) contributing to resistance to third-generation EGFR-TKIs. In the RAS-RTK pathways, *MET* amp was found in 24% of cases, while *ERBB2* amp was noted in 8%. Furthermore, the histological evaluation of tissue samples collected at the time of sequencing showed that 48 patients maintained a diagnosis of adenocarcinoma. In contrast, one patient exhibited a transformation to SCLC. Patient P24 demonstrated a transformation to SCLC with classical *RB1* loss[22]. Furthermore, a *PIK3CB* missense mutation and copy number gains in *NRAS*, *CDK6*, and *MET* were also identified.

An evaluation of the driver mutation landscape analysis for bulk-seq was conducted to understand the molecular alterations associated with resistance, including single nucleotide variants (SNVs) and CNVs. However, no shared common resistance mechanism for specific genes was identified in patients. This underscores the possibility that the *EGFR*-dependent or bypass signaling mechanisms of third-generation EGFR-TKIs may manifest differently across individual patients.

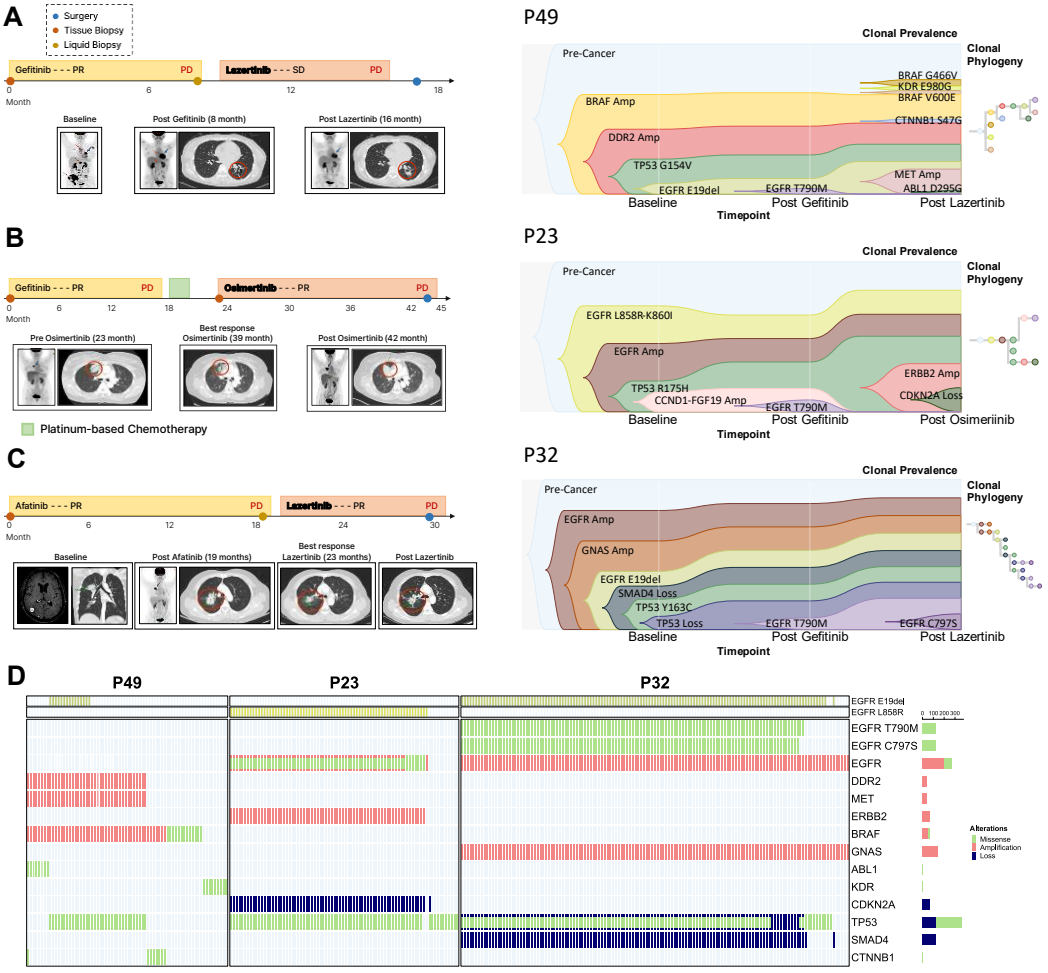

Figure 3. Clonal Evolution of Second line third-generation EGFR-TKIs Resistance using scDNA-seq

A-C. Clonal prevalence and Phylogenetic trees were constructed from bulk-seq and scDNA-seq of baseline, pre- and post-third-generation EGFR-TKIs resistant tumors of patients (A) P49, (B) P23, and (C) P31. SNVs and CNVs in cancer-related genes in fish plots are indicated with the timeline. The clinical timeline from diagnosis of metastatic disease to progression on third-generation EGFR-TKIs for each subject is summarized left each fish plot. sampling timepoints of baseline, post-first-generation EGFR-TKI, and post-third-generation EGFR-TKI tumors are shown for each clinical timeline. D. The oncoplot shows the mutations of each gene in post-third-generation EGFR-TKI

samples from scDNA-seq patients in the study. Mutations are color-coded according to their type. Percentages on the right indicate the prevalence of mutations in each gene among the tumor samples analyzed from each patient. Each column represents a single tumor cell.

Bulk-seq, bulk-sequencing; scDNA-seq, single cell DNA sequencing; CNV, copy number variant; EGFR, epidermal growth factor receptor; SNV, single nucleotide variant; TKI, tyrosine kinase inhibitor; VAF, variant allele frequency.

3.3. The candidate resistance mechanism in bulk sequencing

Although diverse mechanisms contributing to resistance against third-generation EGFR-TKIs have been observed, we focused on the common mechanisms in selected patients. 12.5% of the patients had the *EGFR* C797S mutation in conjunction with the T790M mutation, and the allele frequencies of the T790M and C797S mutations were similar (Figure 2D). This demonstrates the possibility that the *EGFR*-dependent somatic mutation C797S may have been acquired within the *EGFR* T790M tumor clones.

ERBB2 amp was identified in four patients (P17, P19, P23, and P48), of whom P19, P23, and P48 received third-generation EGFR-TKI as second or higher-line treatments. *ERBB2* amp occurred mutually exclusive to *EGFR* T790M in all patients. Additionally, three patients (P17, P19, and P23) co-exhibited *EGFR* amp in bulk-seq (Figure 2A). However, the co-expression of the *ERBB2* amp and *EGFR* amp necessitates further verification in an expanded cohort.

In addition, patients with high tumor purity but low *EGFR* oncogenic mutation variant allele frequency (VAF) after treatment were also identified. We identified 2 patients expected to exhibit similar characteristics by establishing a cutoff of more than 70% for tumor purity and less than 25% for the VAF of the *EGFR* oncogenic mutation (Table 2). In both patients, the treatment was escalated to the 7^{th} line or higher following the administration of third-generation EGFR-TKIs, and they exhibited a shorter progression-free survival (PFS) compared to the other patients (Supplementary Figure 3A, B). This suggests that the genetic heterogeneity of the patients has significant implications for treatment outcomes.

We monitored a patient who experienced progression while receiving EGFR-TKIs. The VAF of *EGFR* oncogenic mutations and other somatic mutations were compared in seven patients through pre- and post-treatment analysis. No trend was observed indicating a decrease in the VAF of EGFR oncogenic mutations with EGFR-TKIs (Figure 2B). Monitoring the VAF of *EGFR* changes during

treatment was challenging, as sampling was only at the time of disease progression. Furthermore, a common trend in CNAs was not identified (Figure 2C). These findings suggest that the results reflect the tumor heterogeneity among individual patients.

Additionally, in the cohort of patients treated with third-generation EGFR-TKI for the second time or more, there were alterations involving three or more mutations, excluding EGFR-activating mutations. This indicates, as previously studied, a higher mutational burden and increased complexity of genetic alterations resulting from drug pressure and subsequent outcomes in advanced stages compared to early-stage NSCLC[23, 24].

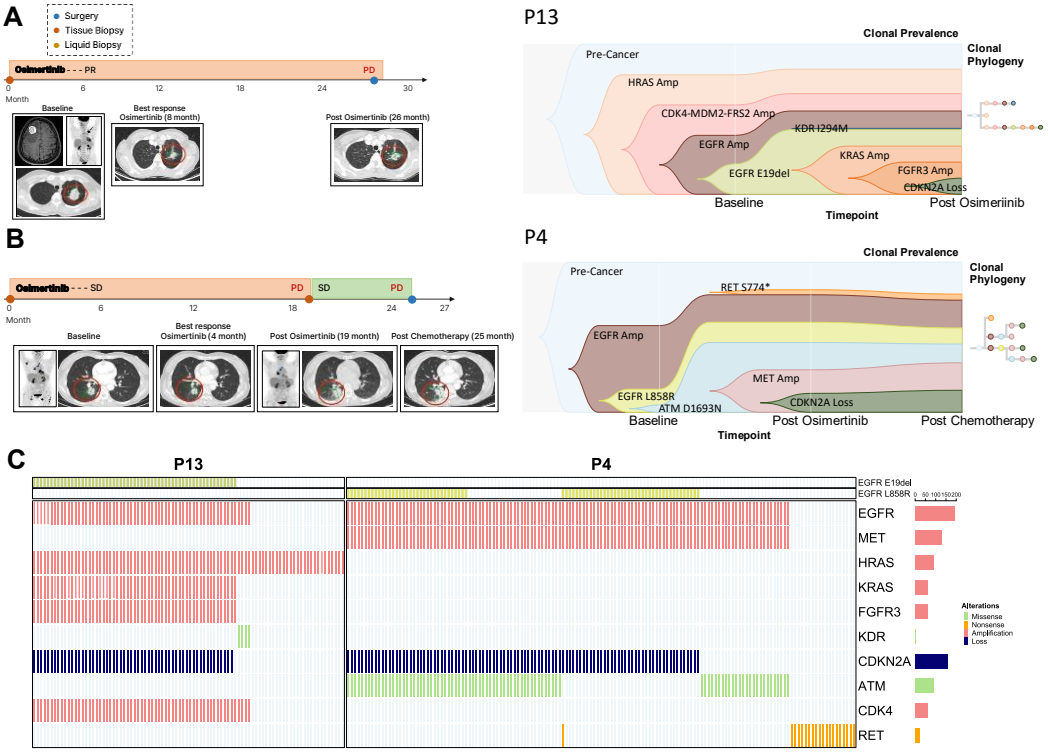

Figure 4. Clonal Evolution of First line third-generation EGFR-TKIs Resistance using scDNA-seq

A-B. Clonal prevalence and Phylogenetic trees were constructed from bulk-seq and scDNA-seq of baseline and post-third-generation EGFR-TKIs resistant tumors of patients (A) P13, and (B) P4. SNVs and CNVs in cancer-related genes in fish plots are indicated with the timeline. The clinical timeline from diagnosis of metastatic disease to progression on third-generation EGFR-TKIs for each subject is summarized left each fish plot. sampling time points of baseline and post-third-generation EGFR-TKI tumors are shown for each clinical timeline. C. The oncoplot shows the mutations of each gene in post-third-generation EGFR-TKI samples from scDNA-seq patients in the study. Mutations are color-coded according to their type. Percentages on the right indicate the prevalence of mutations in each gene among the tumor samples analyzed from each patient. Each column represents a single tumor cell.

Bulk-seq, bulk-sequencing; scDNA-seq, single cell DNA sequencing; CNV, copy number variant; EGFR, epidermal growth factor receptor; SNV, single nucleotide variant; TKI, tyrosine kinase

inhibitor; VAF, variant allele frequency.

3.4. scDNA-seq identified mutually exclusive or acquired clones in third-generation EGFR-TKIs resistance patients.

EGFR-mutant NSCLCs resistant to TKIs exhibit genetic heterogeneity with complex mechanisms[25, 26]; however, little is known about the evolution of these tumors during EGFR-TKI treatment. Based on bulk-seq results, we analyzed fresh tissue samples from five patients to gain insight into clonal evolution during third-generation EGFR-TKI treatment. Three patients had received second-line treatment, while two received first-line therapy with third-generation EGFR-TKIs. scDNA-seq was used for analysis, and bulk-seq was also used for cross-validation. Surgical procedures were performed post-treatment and at progression while on third-generation EGFR-TKIs (Supplementary Figure 2A, B). All patients responded to third-generation EGFR-TKIs with either partial remission (PR) or stable disease (SD). Tissue was collected from patients with oligoprogression through resection, all of whom underwent lung resection surgery. Using scDNA-seq and bulk-seq analysis, we determined the clonal relationships of the clones within the patient. Our clonal evaluation identified subclones within the patients that evolved during treatment (Figures 3 and 4). Oncogenic *EGFR* mutations (such as *EGFR* E19del and L858R) were generally present in most subclones. *TP53* missense mutations were detected at the pre-treatment baseline and continued to be present following third-generation EGFR-TKI treatments. These findings align with those reported in TRACERx, indicating that somatic alterations of *TP53* were predominantly truncal maintained[27]. *TP53* mutations were consistently clonal (P49 *TP53* G154V, P23 *TP53* R175H, and P32 *TP53* Y163C) and were identified in patients receiving third-generation EGFR-TKI as a second-line treatment (Figure 3). The VAF of these mutations increased during TKI treatment, suggesting that they may serve as a resistance mechanism to EGFR-TKIs in selected patients[21, 28].

The *EGFR* T790M mutation, known as the most common resistance mechanism to first- and second-generation EGFR-TKIs, was detected in P49, 23, and 32 before treatment with third-generation EGFR-TKIs. During treatment, patients P49 and P23 exhibited a loss of T790M and did not acquire any additional *EGFR*-dependent mutations. In contrast, Patient P32 maintained the T790M mutation even after third-generation *EGFR*-TKI treatment and acquired the *EGFR* C797S mutation, an *EGFR*-dependent mutation. The VAF of T790M and C797S in bulk-seq and scDNA-seq were

similar (Figure 2D), and scDNA-seq analysis showed that the T790M mutation acquired the C797S mutation within the same cells (Figure 3D).

In contrast, selected patients acquired *EGFR*-independent somatic mutations in oncogenes (P49, *CTNNB1* S47G, *BRAF* G466V, *KDR* E980G, *ABL1* D295G; P13, *KDR* I294M; P4, *RET* S774*), which were characterized by low VAFs and were not clonal with the *EGFR* oncogenic mutation (Figure 3D and 4C). In general, it has been reported that *BRAF* mutations occur mutually exclusive of other known oncogenic driver mutations[29-31], which is consistent with our data. Clinical findings indicate that vemurafenib, a BRAF inhibitor, has no impact on the class III mutation *BRAF* G466V[32], Class III mutations are much more aggressive than class I (*BRAF* V600E) in lung cancer[33]. Furthermore, there have been reports of Class III mutation cell lines exhibiting antagonistic effects when dabrafenib (*BRAF* inhibitor) and trametinib (MEK inhibitor) are combined, and retrospective studies have shown that if triple-targeted treatment is not a *BRAF* class I variant, median progression-free survival (mPFS) was similar in treated and untreated patients[34, 35]. Patient P49 received a combination of gefitinib, dabrafenib, and trametinib following progression on lazertinib, resulting in a PFS of approximately 5 months (Supplement Figure 3A). Moreover, *CTNNB1* S47G mutation has been reported in *EGFR*-mutant NSCLC patients receiving TKI treatment[36]. Alterations in genes associated with the Wingless-related integration site (WNT) signaling pathway may destabilize protein-protein interaction interfaces, potentially indicating a response to targeted therapy[37]. *ABL1* D295G has previously been found in colorectal cancer and lymphoblastic leukemia, and it has been reported to confer resistance to TKIs and imatinib[38]. Furthermore, in P49, the acquired *BRAF* V600E mutation was identified only through bulk-seq, not scDNA-seq. This patient exhibited high tumor purity and a low VAF of the *EGFR* oncogenic mutation in bulk sequencing. These findings highlight increased molecular complexity and tumor heterogeneity associated with TKI resistance[39, 40]. P49 had received over seven lines of treatment after TKI progression, suggesting that adequate cancer suppression had not been achieved due to intra-tumoral heterogeneity.

Overall, *EGFR*-independent acquired somatic mutations have exclusively low VAFs and are distinct from *EGFR* oncogenic mutations. In contrast, *EGFR*-dependent somatic C797S mutations, which have a similar VAF to that of the T790M mutation, tend to accumulate alongside the *EGFR* oncogenic mutation. This data suggests that *EGFR*-dependent somatic mutations arise within *EGFR* oncogenic clones, while *EGFR*-independent somatic mutations occur exclusively. Likewise, effective treatment strategies are necessary to target minor somatic mutation clones in patients

exhibiting high tumor purity and low VAF of *EGFR* oncogenic mutations.

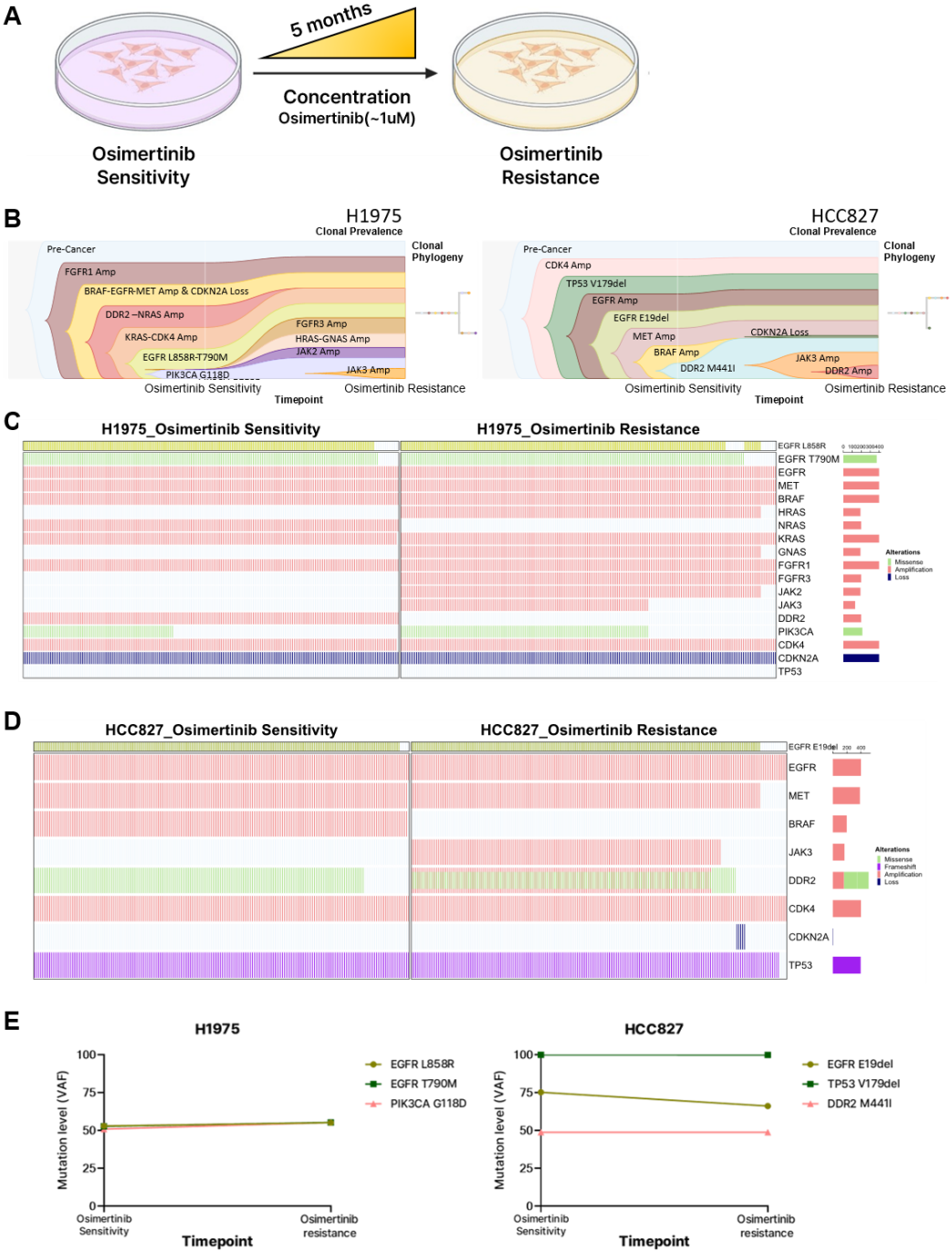

Figure 5. Analysis of Clonal evolution of osimertinib-resistant NSCLC Cell lines.

A. Study Design of osimertinib-resistant cell line establishment. B. Clonal prevalence and Phylogenetic trees were constructed from scDNA-seq of pre-and post-osimertinib resistant cells of H1975 and HCC827. C-D. The oncoplot shows the mutations of each gene in osimertinib sensitivity and osimertinib resistance (C) H1975, H1975OR and (D) HCC827, HCC827OR cell lines from scDNA-seq in the study. Mutations are color-coded according to their type. Percentages on the right indicate the prevalence of mutations in each gene among the tumor cells analyzed from each cell line. Each column represents a single tumor cell. E. Changes in VAFs during osimertinib treatment. The Y-axis indicates VAF for mutations, and the X-axis indicates the timepoints.

scDNA-seq, single cell DNA sequencing; VAF, variant allele frequency; OR, osimertinib resistance.

3.5. scDNA-seq Identified Multiple Copy Number Alterations in Individual Patients

CNAs appeared variably during treatment, with *EGFR* amp commonly occurring earlier in tumor evolution[23]. In selected patients (P13, *KRAS* amp, and *FGFR3* amp; P23, *ERBB2* amp; P49, P4, *MET* amp), changes in CNAs of the RTK/RAS pathway were observed during third-generation EGFR-TKI treatment, and these amps were acquired within the oncogenic *EGFR* mutation clones. As previously reported, the resistance mechanism *ERBB2* amp (P23) occurred mutually exclusive with *EGFR* T790M and was acquired from the EGFR oncogene clone[41, 42]. Moreover, *CDKN2A* loss in the cell cycle pathway (P23, P13, P4) was observed in most patients and was partially acquired in the *EGFR* oncogenic mutation clone. Genetic alterations within the cell cycle pathway of *CDKN2A* loss can co-occur with *EGFR* oncogenic mutation[37, 43]. This change can induce tumor metastasis and limit targeted therapy response, demonstrating a higher proliferative capacity[44].

In addition, it has been previously reported that changes in copy number may appear spatially separate in individuals receiving third-generation EGFR-TKI treatments[21]. Our data indicates that *MET* amp (P49, P4) prominently exhibits spatial clonal heterogeneity. The *ATM* D1693N missense mutation (P4) demonstrates an increase in VAF during treatment (Figure 2C), and *CDKN2A* loss, along with *MET* amp, was observed in *EGFR* wild-type *ATM* missense mutant clones (Figure 4C). This suggests that the CNAs acquired in this clone may be spatially distinct, indicating that the cancer cells can persist without an *EGFR* oncogenic mutation.

In contrast to previously identified resistance mechanisms, *FGFR3* amp occurred in P13. Although

the precise mechanism of *FGFR3* overexpression in NSCLC remains incompletely understood, the dysregulation of *FGFR3* expression has been implicated in the pathogenesis of urothelial bladder cancer[45, 46]. *MYC* was excluded from the analysis due to the limitations of the scDNA-seq panel; however, *MYC* amp was detected in bulk sequencing. *MYC* is essential for directly regulating *FGFR3* expression at the transcriptional level, creating a positive feedback loop between *FGFR3* and *MYC*[47]. The *MYC* transcription factor is a key downstream effector of *FGFR* signaling and has been shown to mediate tumor formation in cancer cells with various *FGFR* abnormalities, including bladder cancer[46]. In addition, tumors with *FGFR* amp have been reported to upregulate the *MYC* and *MTOR* oncogenic pathways compared to other tumors[48]. In summary, it is anticipated that *MYC* and *FGFR3* amps may affect resistance to third-generation EGFR-TKIs in P13 although further experiments are necessary to validate this hypothesis.

Somatic mutations and multiple CNAs occur at distinct spatial and temporal stages during treatment with third-generation EGFR-TKIs. Similar to the previous bulk-seq cohort, no shared mechanism has been identified in all patients. This demonstrates that resistance to third-generation EGFR TKIs arises due to various mechanisms, unlike the *EGFR* T790M mutation known for conferring resistance to first-generation EGFR TKIs. Furthermore, it illustrates the differences in drug pressure among patients receiving the same third-generation EGFR-TKI and highlights the absence of comprehensive genomic profiling.

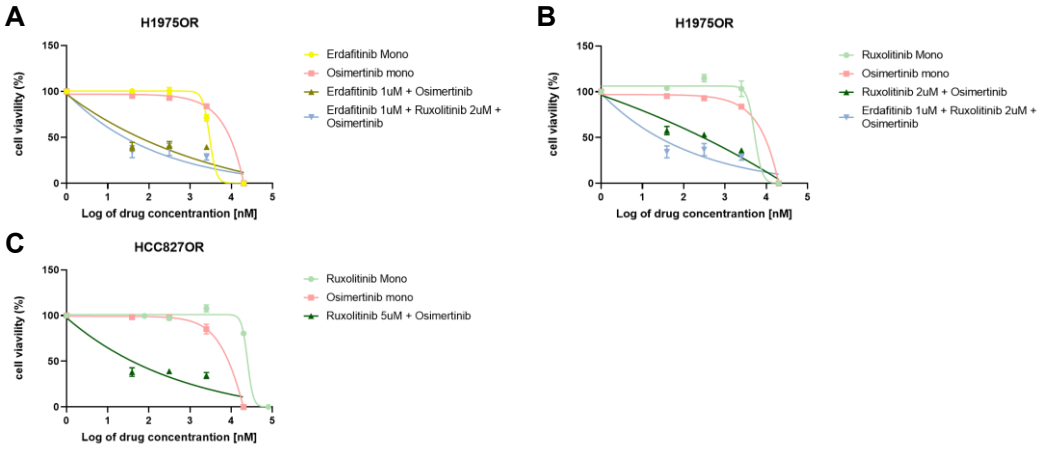

Figure 6. Overcoming osimertinib resistance mechanisms by combination treatment

A-C. Cell viability assessment shows synergistic inhibition of osimertinib resistance cell lines. H1975OR cells were treated with increasing concentrations of osimertinib, (A) erdafitinib, and (B) ruxolitinib mono or in combination. (C) HCC827OR cells were treated with increasing concentrations of osimertinib, and ruxolitinib mono or in combination.

OR, osimertinib resistance.

3.6. Analysis of Resistance Mechanisms in In vitro and Treatment Strategies to Overcome Resistance.

We established osimertinib-resistant in vitro models using the NCI-H1975 (H1975) and HCC827 cell lines (Figure 5A, Supplementary Figures 4A, B). These cell lines feature different *EGFR* oncogenic mutation backgrounds and are initially sensitive to osimertinib. The H1975 cell line harbors the *EGFR* L858R/T790M double mutation, while the HCC827 cell line contains the *EGFR* E19dels. Osimertinib-resistant cell lines were induced by gradually increasing the drug concentration from 10nM to 1μM. After five months, we established the osimertinib-resistant cell lines, labeled HCC827OR and H1975OR. To gain further insight into the resistance mechanisms and clonal evolution associated with third-generation EGFR-TKIs, we also performed scDNA-seq on both the parental and osimertinib-resistant cell lines. The previously identified *TP53* R273H mutation in H1975 was not detected in the SNV analysis, as the panel used does not cover this specific mutation region.

Low VAF *EGFR*-independent somatic mutations were not observed due to the cell line's homogeneity; only CNV alterations were found. In the analysis of CNAs, both cell lines showed that the *EGFR* amp originated from the parent cell lines (Figures 5C and 5D). In H1975, osimertinib resistance-emergent CNAs, including *FGFR3* amp, were acquired in the *EGFR* oncogenic mutation clone, and HCC827, *CDKN2A* loss was partially acquired in the *EGFR* oncogenic mutation clone. These CNAs are consistent with the findings from scDNA-seq in patients. Additionally, H1975OR exhibited *HRAS*, *GNAS*, and *JAK2* amps, with the *JAK3* amp appearing to be partially acquired in the *EGFR* oncogenic clones (Figure 5C). In HCC827, amps of *JAK3* and *DDR2* were also found to be partially acquired in the *EGFR* oncogenic clones (Figure 5D). These changes in the cell lines demonstrate that alterations in copy number due to third-generation EGFR-TKI can vary from cell to cell, experimentally supporting the findings of different CNAs in spatially separate individuals in scDNA-seq patients.

To investigate the roles of *FGFR3* and *JAK3* amps in osimertinib resistance, we tested whether a combination therapy of osimertinib with erdafitinib (*FGFR3* inhibitor) and ruxolitinib (*JAK3* inhibitor) could overcome resistance. H1975OR cells were treated with osimertinib, erdafitinib, and ruxolitinib either alone or in combination at increasing concentrations. The combination of osimertinib with erdafitinib or ruxolitinib allowed for the restoration of sensitivity in the resistant cell line (Figure 6A, B). Furthermore, the triple of osimertinib, erdafitinib, and ruxolitinib produced a more pronounced effect than the dual combination; however, additional studies on this triple combination therapy are warranted. Likewise, adding ruxolitinib to HCC827OR reinstated sensitivity to osimertinib (Figure 6C). These results underscore the importance of combination therapy in restoring osimertinib sensitivity when bypass mechanisms arise in resistant cells.

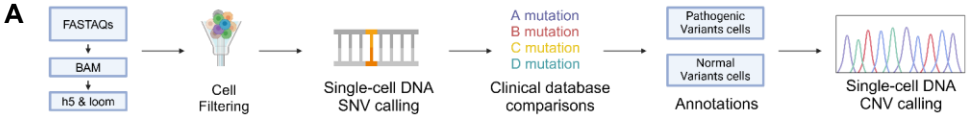

Supplementary Figure 1. Analysis flow of scDNA-seq

A. Summary of the scDNA-seq analysis.

scDNA-seq, single cell DNA sequencing.

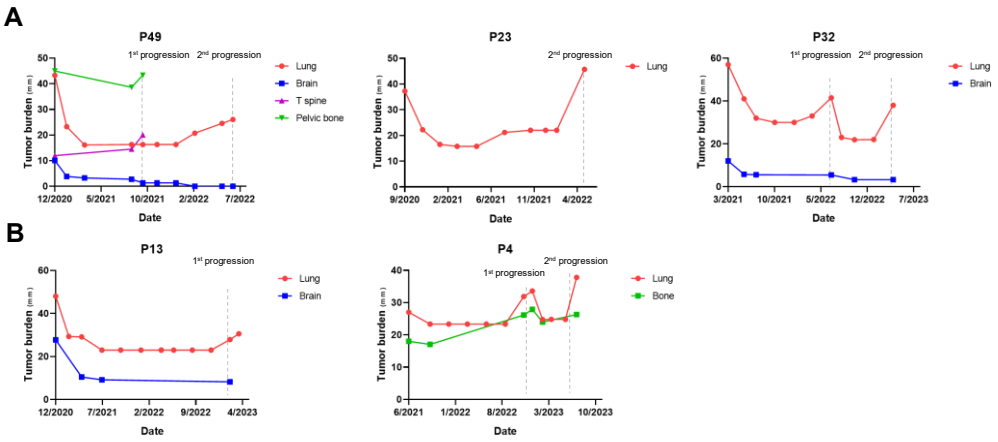

Supplementary Figure 2. Changes in Tumor Burden with EGFR-TKIs

A. Changes in patient Tumor Burden during first-generation EGFR-TKIs and third-generation EGFR-TKIs treatment. B. Changes in patient Tumor burden during third-generation EGFR-TKIs. EGFR, epidermal growth factor receptor; TKI, tyrosine kinase inhibitor.

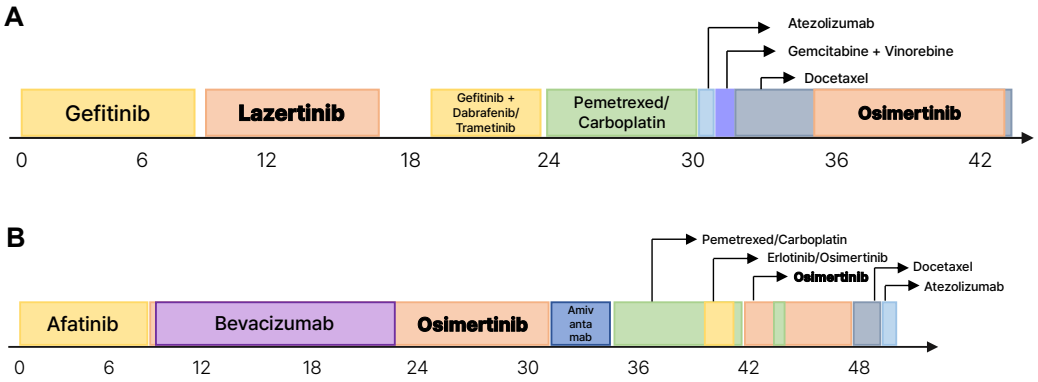

Supplementary Figure 3. Clinical timeline of P40 and P49

A-B. Clinical timeline from diagnosis of metastatic disease to progression on treatment (A) P49, (B) P40.

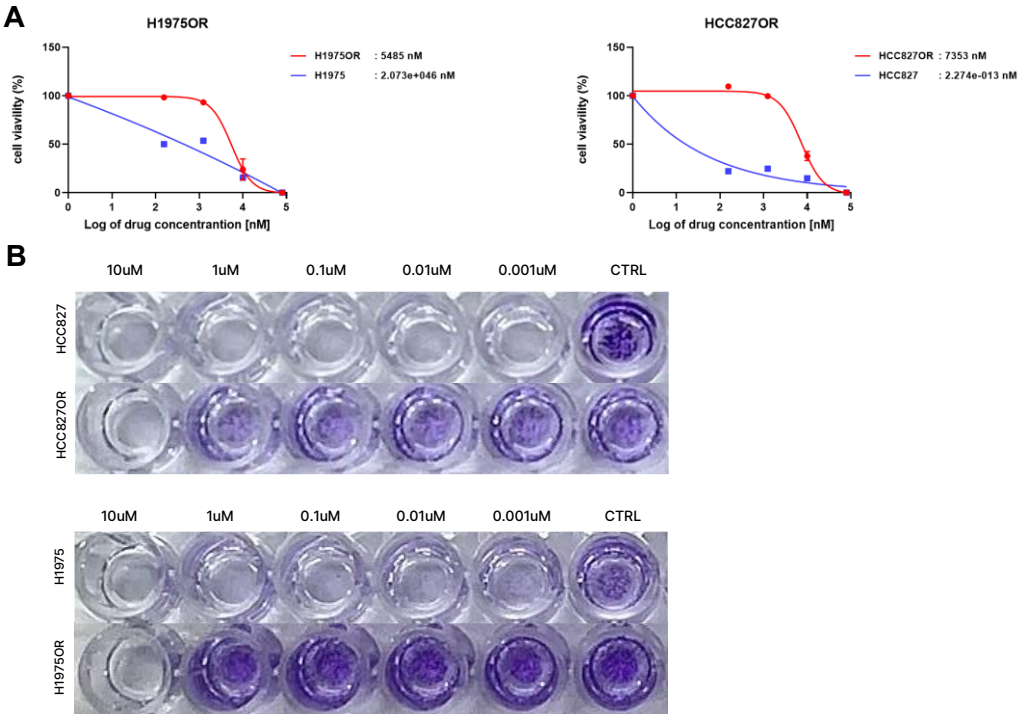

Supplement Figure 4. Establishment of third-generation EGFR-TKIs resistant NSCLC Cell Lines.

A. Cells were incubated with various concentrations of osimertinib for 72h. The antiproliferative effects of osimertinib in H1975, H1975OR, HCC827, and HCC827OR cells were evaluated by WST assay. B. Cells were exposed to osimertinib for 72h. Then, cells were fixed with methanol and stained with crystal violet. The cells were photographed and representative images were exhibited. OR, osimertinib resistance; WST, water-soluble tetrazolium salts.

Table 1. Clinical characteristics of all patients.

Characteristics	Total (N=49)		1st Line(N=17)		≥2nd Line(N=32)	
		%		%		%
Gender						
Male (M)	16	32.7	4	23.5	12	37.5
Female (F)	33	67.3	13	76.5	20	62.5
Age (years)						
Median	61		61		61	
Range	33-81		44-81		33-78	
Smoking						
Current	3	6.1	2	11.8	1	3.1
Former	10	20.4	2	11.8	8	25.0
Never	36	73.5	13	76.5	23	71.9
Histological type						
LUAD	49	100.0	17	100.0	32	100.0
LSQC		-		-		-
Baseline EGFR Mutation						
EGFR E19del	24	49.0	6	35.3	18	56.3
EGFR L858R	25	51.0	11	64.7	14	43.8
Best Response						
CR		-		-		-
PR	22	44.9	11	64.7	11	34.4
SD	27	55.1	6	35.3	21	65.6
PD		-		-		-
Stage						
I	2	4.1		-	2	6.3
II		-		-		-
III	5	10.2	2	11.8	3	9.4
IV	42	85.7	15	88.2	27	84.4
ECOG						
0	27	55.1	12	70.6	15	46.9
1	22	44.9	5	29.4	17	53.1

Third-generation EGFR-TKI						
Osimertinib	47	95.9	17	100.0	30	93.8
Lazertinib	2	4.1		0.0	2	6.3
Prior EGFR-TKI						
Afatinib	12	24.5		-	12	37.5
Erlotinib	3	6.1		-	3	9.4
Gefitinib	17	34.7		-	17	53.1
Line of third-generation EGFR-TKI						
1	17	34.7	17	100.0		-
2	23	46.9		-	23	71.9
3	6	12.2		-	6	18.8
≥4	3	6.1		-	3	9.4
Metastasis prior to third-generation EGFR-TKI						
Brain metastasis	29	59.2	11	64.7	18	56.3
No Brain metastasis	20	40.8	6	35.3	14	43.8

NSCLC, non-small cell lung cancer; EGFR, epidermal growth factor receptor; TKI, tyrosine kinase inhibitor; ECOG, eastern cooperative oncology group performance status; LUAD, lung adenocarcinoma; LUSC, lung squamous cell carcinoma; CR, complete response; PR, partial response; SD, stable response; PD, progression disease.

Table 2. Patient's tumor purity and EGFR oncogenic variant allele frequencies

Patients_No.	Tumor purity	EGFR oncogenic mutation VAF(%)
P1	0.8	59.968
P2	0.8	25.152
P3	0.35	19.908
P4	0.5	5.525
P5	0.3	6.603
P6	0.3	6.366
P7	0.2	5.324
P8	0.5	13.32
P9	0.2	3.632
P10	0.3	7.734
P11	0.4	10.08
P12	0.3	12.474
P13	0.3	7.281
P14	0.6	17.43
P15	0.5	34.445
P16	0.1	0.74
P17	0.5	24.58
P18	0.5	47.935
P19	0.85	80.9115
P20	0.75	34.3125
P21	0.1	0.218
P22	0.3	13.254
P23	0.3	11.85
P24	0.8	33.608
P25	0.7	59.612
P26	0.2	5.34
P27	0.6	9.384
P28	0.25	1.59
P29	0.35	1.414

P30	0.1	0.498
P31	0.15	3.8115
P32	0.7	46.62
P33	0.8	27.904
P34	0.4	12.72
P35	0.2	2.852
P36	0.4	35.068
P37	0.3	15.99
P38	0.45	36.513
P39	0.35	13.3945
P40	0.9	21.069
P41	0.7	64.043
P42	0.3	3.174
P43	0.4	16.792
P44	0.2	9.056
P45	0.3	9.543
P46	0.85	50.4985
P47	0.3	5.388
P48	0.8	40.504
P49	0.7	14.448

EGFR, epidermal growth factor receptor; VAF, variant allele frequency.

IV. Discussion

Third-generation EGFR-TKIs have revolutionized the treatment of *EGFR*-mutant NSCLCs. Despite their significant initial efficacy, the emergence of resistance mechanisms and the increase in tumor heterogeneity present inevitable limitations to treatment effectiveness. Consequently, we faced the challenge of selecting next-line treatment options in the context of resistance. This study contributes to understanding the necessity of combination therapy, describing the genetic heterogeneity and clonal evolution linked to resistance mechanisms against third-generation EGFR-TKIs in patients with EGFR-mutant NSCLC and in vitro contexts.

Although the mechanisms underlying resistance to third-generation EGFR-TKIs have been reported, whether these driver mutations coexist within a single cell remains. Bulk sequencing has confirmed inter-patient heterogeneity, and to address the complex heterogeneity of TKI-resistant tumors, we conducted clonal evolution analyses using scDNA-seq. While it is believed that oncogenic mutations occur in *EGFR*-mutant NSCLC within the same cell, we have demonstrated that the acquisition of these mutations varies depending on the type, such as *EGFR*-dependent or bypass mutations.

The scDNA-seq analysis of third-generation EGFR-TKIs highlighted the mutual exclusivity between activated *EGFR* mutations. It independently acquired minor mutations in patients P49 (*CTNNB1* S47G, *BRAF* G466V, *KDR* E980G, *ABL1* D295G), P13 (*KDR* I294M), and P4 (*RET* S774*). Notably, patient P49 showed the emergence of *EGFR*-independent somatic mutation clones that outnumbered the existing *EGFR* oncogenic cells, being mutually exclusive to the *EGFR* oncogenic mutation. The findings suggest that minor subclones with these mutations may play a role in EGFR-TKI resistance across a wider range of cancer cells. Additionally, the mutually exclusive occurrence of *BRAF* G466V and *EGFR* E19del mutations in patient P49 and the lack of *BRAF* V600E detection in single-cell analyses may be attributed to intra-tumoral heterogeneity. Conversely, P32 illustrated that *EGFR* C797S was acquired in the *EGFR* T790M clone, showing that *EGFR*-dependent mutations can accumulate alongside *EGFR* oncogenic mutations within the same cells. Understanding these changes at the single-cell level is significant for clinical implications practice. Research targeting resistance mechanisms continues to progress[11]; however, there is a lack of evidence suggesting clinical benefits. Experiments on osimertinib-resistant cell lines show that combination therapy can reactivate sensitivity to osimertinib, implying that further combination strategies should be tested for clinical efficacy advantages.

In conclusion, our study employing scDNA-seq and bulk-seq in patients, along with osimertinib-resistant NSCLC cell lines, reveals genetic heterogeneity and clonal evolution in advanced *EGFR*-mutated lung cancer treated with third-generation EGFR-TKIs. Most patients on these treatments displayed more than two resistance mechanisms, which varied among individuals, even under the same drug pressure. Furthermore, scDNA-seq showed that mutations can differ within the same patient, indicating that the mutations caused by third-generation EGFR-TKIs contribute to intratumor heterogeneity on a cellular level. Our results suggest that combination therapy might be essential to overcome acquired resistance, emphasizing the ongoing challenge of identifying tailored optimal treatments for each patient. Nonetheless, the feasibility of combination therapy was not assessed in the in vivo study. Determining the best treatment strategy will require prospective clinical trials, either in vivo or based on biomarkers trials.

References

1 Oliver AL. Lung cancer: epidemiology and screening. Surgical Clinics 2022; 102 (3): 335-344.
2 Jänne PA, Engelman JA, Johnson BE. Epidermal growth factor receptor mutations in non–small-cell lung cancer: Implications for treatment and tumor biology. Journal of clinical oncology 2005; 23 (14): 3227-3234.
3 Rajaram P, Chandra P, Ticku S et al. Epidermal growth factor receptor: Role in human cancer. Indian Journal of Dental Research 2017; 28 (6): 687-694.
4 Soria J-C, Ohe Y, Vansteenkiste J et al. Osimertinib in untreated EGFR-mutated advanced non–small-cell lung cancer. New England journal of medicine 2018; 378 (2): 113-125.
5 Ramalingam SS, Vansteenkiste J, Planchard D et al. Overall Survival with Osimertinib in Untreated, EGFR-Mutated Advanced NSCLC. N Engl J Med 2020; 382 (1): 41-50.
6 Cho BC, Ahn MJ, Kang JH et al. Lazertinib Versus Gefitinib as First-Line Treatment in Patients With EGFR-Mutated Advanced Non-Small-Cell Lung Cancer: Results From LASER301. J Clin Oncol 2023; 41 (26): 4208-4217.
7 Oxnard GR, Hu Y, Mileham KF et al. Assessment of resistance mechanisms and clinical implications in patients with EGFR T790M–positive lung cancer and acquired resistance to osimertinib. JAMA oncology 2018; 4 (11): 1527-1534.
8 Leonetti A, Sharma S, Minari R et al. Resistance mechanisms to osimertinib in EGFR-mutated non-small cell lung cancer. British journal of cancer 2019; 121 (9): 725-737.
9 Chmielecki J, Gray JE, Cheng Y et al. Candidate mechanisms of acquired resistance to first-line osimertinib in EGFR-mutated advanced non-small cell lung cancer. Nat Commun 2023; 14 (1): 1070.
10 Gomatou G, Syrigos N, Kotteas E. Osimertinib Resistance: Molecular Mechanisms and Emerging Treatment Options. Cancers (Basel) 2023; 15 (3).
11 Yu HA, Goldberg SB, Le X et al. Biomarker-Directed Phase II Platform Study in Patients With EGFR Sensitizing Mutation-Positive Advanced/Metastatic Non-Small Cell Lung Cancer Whose Disease Has Progressed on First-Line Osimertinib Therapy (ORCHARD). Clin Lung Cancer 2021; 22 (6): 601-606.
12 Hartmaier RJ, Markovets AA, Ahn MJ et al. Osimertinib + Savolitinib to Overcome Acquired MET-Mediated Resistance in Epidermal Growth Factor Receptor-Mutated, MET-Amplified Non-Small Cell Lung Cancer: TATTON. Cancer Discov 2023; 13 (1): 98-113.
13 Wu YL, Guarneri V, Voon PJ et al. Tepotinib plus osimertinib in patients with EGFR-mutated non-small-cell lung cancer with MET amplification following progression on first-line osimertinib (INSIGHT 2): a multicentre, open-label, phase 2 trial. Lancet Oncol 2024; 25 (8): 989-1002.
14 Wang Z, Wu YL. Re-emerging C797S In Trans and Rechallenge of Osimertinib With Erlotinib. J Thorac Oncol 2019; 14 (4): e81-e82.
15 Lim ZF, Ma PC. Emerging insights of tumor heterogeneity and drug resistance mechanisms in lung cancer targeted therapy. J Hematol Oncol 2019; 12 (1): 134.
16 Kohsaka S, Petronczki M, Solca F, Maemondo M. Tumor clonality and resistance mechanisms in EGFR mutation-positive non-small-cell lung cancer: implications for therapeutic sequencing. Future Oncol 2019; 15 (6): 637-652.
17 Quang D, Chen Y, Xie X. DANN: a deep learning approach for annotating the pathogenicity of genetic variants. Bioinformatics 2015; 31 (5): 761-763.

18 Kopanos C, Tsiolkas V, Kouris A et al. VarSome: the human genomic variant search engine. Bioinformatics 2019; 35 (11): 1978-1980.
19 Borsi E, Vigliotta I, Poletti A et al. Single-Cell DNA Sequencing Reveals an Evolutionary Pattern of CHIP in Transplant Eligible Multiple Myeloma Patients. Cells 2024; 13 (8).
20 Bruno S, Borsi E, Patuelli A et al. Tracking Response and Resistance in Acute Myeloid Leukemia through Single-Cell DNA Sequencing Helps Uncover New Therapeutic Targets. Int J Mol Sci 2024; 25 (18).
21 Roper N, Brown A-L, Wei JS et al. Clonal Evolution and Heterogeneity of Osimertinib Acquired Resistance Mechanisms in EGFR Mutant Lung Cancer. Cell Reports Medicine 2020; 1 (1): 100007.
22 Niederst MJ, Sequist LV, Poirier JT et al. RB loss in resistant EGFR mutant lung adenocarcinomas that transform to small-cell lung cancer. Nat Commun 2015; 6: 6377.
23 Jamal-Hanjani M, Wilson GA, McGranahan N et al. Tracking the Evolution of Non-Small-Cell Lung Cancer. N Engl J Med 2017; 376 (22): 2109-2121.
24 Stephan-Falkenau S, Streubel A, Mairinger T et al. Landscape of Genomic Alterations and PD-L1 Expression in Early-Stage Non-Small-Cell Lung Cancer (NSCLC)-A Single Center, Retrospective Observational Study. Int J Mol Sci 2022; 23 (20).
25 Lee JK, Lee J, Kim S et al. Clonal History and Genetic Predictors of Transformation Into Small-Cell Carcinomas From Lung Adenocarcinomas. J Clin Oncol 2017; 35 (26): 3065-3074.
26 Nahar R, Zhai W, Zhang T et al. Elucidating the genomic architecture of Asian EGFR-mutant lung adenocarcinoma through multi-region exome sequencing. Nat Commun 2018; 9 (1): 216.
27 Al Bakir M, Huebner A, Martínez-Ruiz C et al. The evolution of non-small cell lung cancer metastases in TRACERx. Nature 2023; 616 (7957): 534-542.
28 Vokes NI, Chambers E, Nguyen T et al. Concurrent TP53 Mutations Facilitate Resistance Evolution in EGFR-Mutant Lung Adenocarcinoma. J Thorac Oncol 2022; 17 (6): 779-792.
29 Baik CS, Myall NJ, Wakelee HA. Targeting BRAF-Mutant Non-Small Cell Lung Cancer: From Molecular Profiling to Rationally Designed Therapy. Oncologist 2017; 22 (7): 786-796.
30 Negrao MV, Raymond VM, Lanman RB et al. Molecular Landscape of BRAF-Mutant NSCLC Reveals an Association Between Clonality and Driver Mutations and Identifies Targetable Non-V600 Driver Mutations. J Thorac Oncol 2020; 15 (10): 1611-1623.
31 Schaufler D, Ast DF, Tumbrink HL et al. Clonal dynamics of BRAF-driven drug resistance in EGFR-mutant lung cancer. NPJ Precis Oncol 2021; 5 (1): 102.
32 Mazieres J, Cropet C, Montané L et al. Vemurafenib in non-small-cell lung cancer patients with BRAF(V600) and BRAF(nonV600) mutations. Ann Oncol 2020; 31 (2): 289-294.
33 Dagogo-Jack I, Martinez P, Yeap BY et al. Impact of BRAF Mutation Class on Disease Characteristics and Clinical Outcomes in BRAF-mutant Lung Cancer. Clin Cancer Res 2019; 25 (1): 158-165.
34 Bracht JWP, Karachaliou N, Bivona T et al. BRAF Mutations Classes I, II, and III in NSCLC Patients Included in the SLLIP Trial: The Need for a New Pre-Clinical Treatment Rationale. Cancers (Basel) 2019; 11 (9).
35 Li Y, Zeng H, Qi C et al. Features and efficacy of triple-targeted therapy for patients with EGFR-mutant non-small-cell lung cancer with acquired BRAF alterations who are resistant to epidermal growth factor receptor tyrosine kinase inhibitors. ESMO Open 2024; 9 (10): 103935.
36 Jin Y, Shi X, Zhao J et al. Mechanisms of primary resistance to EGFR targeted therapy in advanced lung adenocarcinomas. Lung Cancer 2018; 124: 110-116.
37 Blakely CM, Watkins TBK, Wu W et al. Evolution and clinical impact of co-occurring

genetic alterations in advanced-stage EGFR-mutant lung cancers. Nat Genet 2017; 49 (12): 1693-1704.
38 Kovaleva V, Geissler AL, Lutz L et al. Spatio-temporal mutation profiles of case-matched colorectal carcinomas and their metastases reveal unique de novo mutations in metachronous lung metastases by targeted next generation sequencing. Mol Cancer 2016; 15 (1): 63.
39 Aran D, Sirota M, Butte AJ. Systematic pan-cancer analysis of tumour purity. Nat Commun 2015; 6: 8971.
40 Chen J, Facchinetti F, Braye F et al. Single-cell DNA-seq depicts clonal evolution of multiple driver alterations in osimertinib-resistant patients. Ann Oncol 2022; 33 (4): 434-444.
41 Takezawa K, Pirazzoli V, Arcila ME et al. HER2 amplification: a potential mechanism of acquired resistance to EGFR inhibition in EGFR-mutant lung cancers that lack the second-site EGFRT790M mutation. Cancer Discov 2012; 2 (10): 922-933.
42 Planchard D, Loriot Y, André F et al. EGFR-independent mechanisms of acquired resistance to AZD9291 in EGFR T790M-positive NSCLC patients. Ann Oncol 2015; 26 (10): 2073-2078.
43 Jiang J, Gu Y, Liu J et al. Coexistence of p16/CDKN2A homozygous deletions and activating EGFR mutations in lung adenocarcinoma patients signifies a poor response to EGFR-TKIs. Lung Cancer 2016; 102: 101-107.
44 Volta F, La Monica S, Leonetti A et al. Intrinsic Resistance to Osimertinib in EGFR Mutated NSCLC Cell Lines Induced by Alteration in Cell-Cycle Regulators. Target Oncol 2023; 18 (6): 953-964.
45 Ascione CM, Napolitano F, Esposito D et al. Role of FGFR3 in bladder cancer: Treatment landscape and future challenges. Cancer Treat Rev 2023; 115: 102530.
46 Bogale DE. The roles of FGFR3 and c-MYC in urothelial bladder cancer. Discov Oncol 2024; 15 (1): 295.
47 Mahe M, Dufour F, Neyret-Kahn H et al. An FGFR3/MYC positive feedback loop provides new opportunities for targeted therapies in bladder cancers. EMBO Mol Med 2018; 10 (4).
48 Roussot N, Lecuelle J, Dalens L et al. FGF/FGFR genomic amplification as a predictive biomarker for immune checkpoint blockade resistance: a short report. J Immunother Cancer 2023; 11 (10).

Abstract in Korean

비소세포 폐암에서 단일 세포 DNA 시퀀싱을 이용한 3세대 EGFR-TKI 내성 클론 규명

표적 치료제인 3세대 EGFR-티로신 키나아제 저해제는 EGFR 돌연변이 비소세포폐암 환자의 예후를 상당히 개선했지만, 내성 문제는 계속해서 발생하고 있습니다. 대표적으로 *MET*, *ERBB2*의 유전자 증폭과 *EGFR* C797S와 같은 변이가 보고되었으며, 내성 기전이 상호 배타적으로 발생하는지, 혹은 기존 EGFR 발암성 변이에 계속 획득되는지에 대한 논쟁은 계속되고 있습니다. 우리는 차세대 염기서열 분석을 사용하여 진행성 *EGFR* 돌연변이 NSCLC 환자 49명을 대상으로 유전적 이질성을 조사했습니다. 내성 관련 돌연변이와 활성화 *EGFR* 돌연변이가 단일 암세포 내에 공존하는지 또는 별개의 세포 집단에서 발생하는지 확인하기 위해 3세대 EGFR-TKI에 대한 질병 진행 환자 5명의 종양 샘플에 대해 단일 세포 DNA 시퀀싱(scDNA-seq)을 수행했습니다. 또한 오시머티닙 내성 세포주를 확립하고 환자와 같은 패널을 사용해 scDNA-seq를 진행했습니다. 확인된 돌연변이는 시험관 내 실험을 통해 기능적으로 특성화되었습니다. 단일세포 분석 결과, *EGFR* 발암성 돌연변이 내에서 *EGFR* 의존적 체세포 변이가 발생하는 반면, *EGFR* 비의존적 변이는 변이 대립 유전자 빈도가 낮고 *EGFR* 발암성 돌연변이와 상호 배타적으로 나타났습니다. 또한, 제3세대 EGFR-티로신 키나아제 저해제 치료 중 서로 다른 시점과 공간에서 체세포 변이와 다중 복제수 변이가 나타났습니다. 이 연구는 3세대 EGFR-티로신 키나아제 저해제에 대한 내성과 관련된 종양 세포의 유전적 이질성, 클론 진화 및 공간 분포 패턴을 강조합니다. 이러한 발견은 *EGFR* 돌연변이 폐암 환자 관리에서 병용 요법 강화에 대한 근거를 제공합니다.

핵심되는 말 : 비소세포폐암, 단일 세포 DNA 시퀀싱